Position-sensitive device

Bodo Kaiser

Ludwig-Maximilians-Universität München

bodo.kaiser@physik.uni-muenchen.de

April 17, 2019

Contents

1 Introduction

We define a position-sensitive device as a device that converts the center of mass of an input optical signal into an electrical output. The present document is meant to summarize the theory required to design such a position-sensitive device.

Position-sensitive devices are used in a wide range of industrial and commercial applications, including displacement sensing and beam alignment, see Ref. [1, p. 22]. In our case, we were interested in the application of the position-sensitive device for beam pointing alignment. Beam pointing refers to the spatial focus of a laser beam and can change through, for instance, thermal and mechanical effects. Uncompensated changes in beam alignment can quickly degrade the overall performance of an optical system. It is, therefore, crucial to align the beam pointing to ensure proper operation of the optical system at hand. Using a position-sensitive device for monitoring the beam pointing as part of a feedback loop, would allow for automatization of this otherwise cumbersome work.

This document is organized as follows. The first section gives an overview of the design requirements imposed upon our position-sensitive device. In the second section, we summarize the physical theory behind the position-sensitive detector and discuss its electrical properties. In the third section, we dive into the theory of operational amplifier as a front-end for the position-sensitive detector.

2 Requirements

The device should be powered by a dual voltage supply of 15 V using a 4 pin LEMO connector. The components on the printed circuit board should be assembled using surface-mount technology. The device including casing should have a width below 8 cm and a height below 20 cm, preferably smaller, such that it can be integrated easily into existing optical setups. The optical detector should be located as close to the bottom of the device as possible, as it allows greater height compatibility.

The spatial resolution of the center of mass of the incident light should be about 1 µm. Offset errors are tolerable as long as precision is high. We aim for a signal bandwidth of 10 kHz. The radiant flux of the incident light should be in the microwatt range.

3 Position-sensitive detector

3.1 Transverse photoeffect

The purpose of the following section is to recall the mechanics of the (transverse) photoeffect observed in an illuminated p-n junction. Figures and the description thereof is largely based on Ref. [2]. A subtle difference in the depicted figures and the figures of Ref. [2] is that we exchanged the order of p- and n-type semiconductors. We found this order to be more intuitive when referring to a p-n junction.

Figure 1 shows a separated p- and n-type semiconductor. In the upper half, we see an illustration of the p- and n-type semiconductor with their respective mobile charge carriers. The p-type semiconductor has an excess of positive charge carriers (holes) which are depicted as white circles. The n-type semiconductor has an excess of negative charge carriers (electrons) which are depicted as black circles. The excess charge carriers form due to the implantation of acceptor and donator ions. These are depicted as circles with plus and minus sign in Figure 1. The implanted ions have more or fewer electrons than the atoms of the semiconductor material. Therefore donating an electron or accepting an electron and effectively forming a hole as an absence of negative charge.
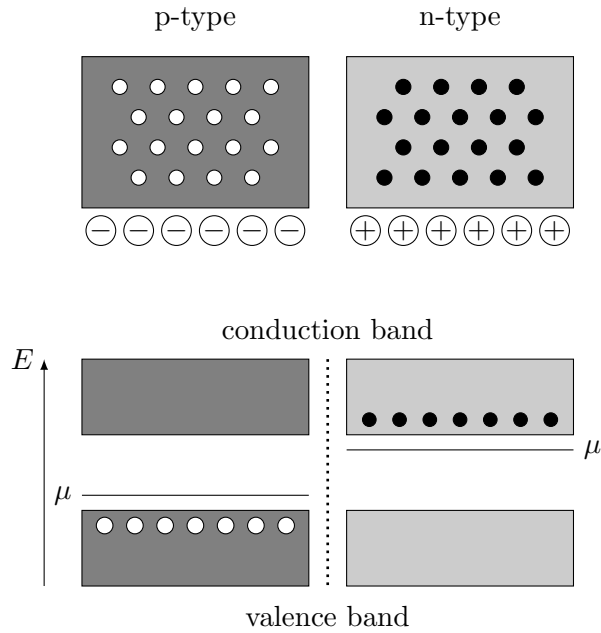

Figure 1: Separated p- and n-type semiconductor with holes (white) and electrons (black).

The lower half of Figure 1 shows the energy band structure of both p- and n-type semi-conductor. The lower energy band represents the valence band made up of the electrons that are tightly bound to a single atomic core. The upper energy band represents the conduction band made up of electrons that are are not bound to a single atomic core but shared across the lattice. Charge carriers in the conduction band can move freely and thereby contribute to the conductivity of the material. For an undoped (intrinsic) semiconductor the chemical potential is in the center of the band gap between the conduction and valence band. Through doping, the chemical potential is shifted in the p- and n-type semiconductor. In the p-type semiconductor, acceptor ions can take up electrons from the conduction band, thereby decreasing the chemical potential. In the n-type semiconductor, donator ions contribute electrons to the conduction band, thereby increasing the chemical potential.
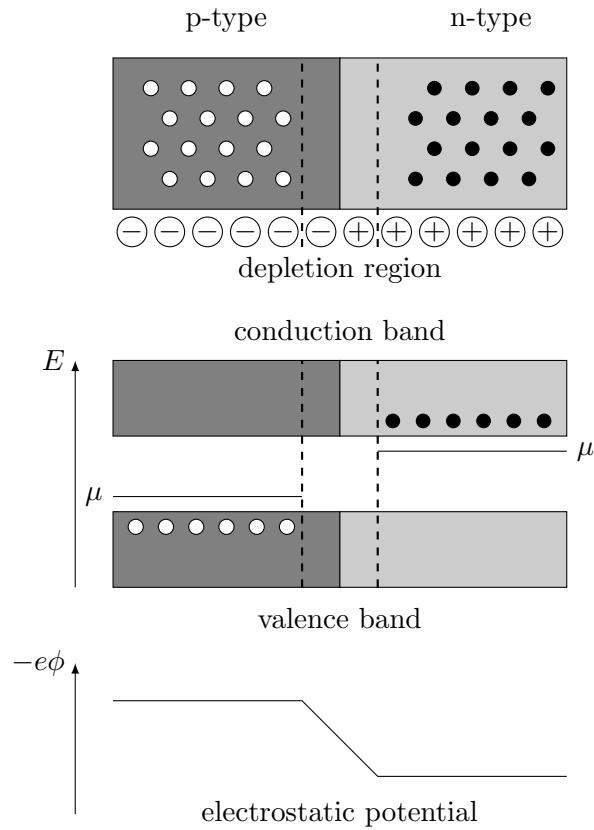

Figure 2: Combined p- and n-type semiconductor with holes (white) and electrons (black).

In Figure 2 the p- and n-type semiconductor are brought into contact with each other, forming a p-n junction. In close proximity of the junction holes and energies recombine due to a diffusion process, leaving an electrically charged area. The electrically charged

area creates an electrostatic potential across the junction as illustrated in the lower part of Figure 2. We refer to this area as the depletion region. In Figure 2 the depletion region expands between the dashed lines around the junction.
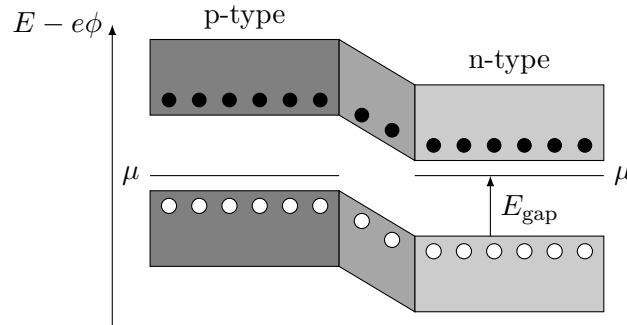

Figure 3: Energy bands of the p-n junction.

The energy band diagram in Figure 3 accounts for the shift in energy due to the electrostatic potential. The chemical potentials of both sides of the junction are now aligned. The energy required to excite an electron on the p-type side from the valence to the conduction band and the energy required to excite a hole from the conduction to the valence band are equal to the band gap of the semiconductor.

If one applies a reverse bias voltage across the p-n junction, the effective energy gap between conduction and valence band is reduced, the electrostatic potential increases and the depletion region broadens. The situation of an applied reverse voltage is depicted in Figure 4.
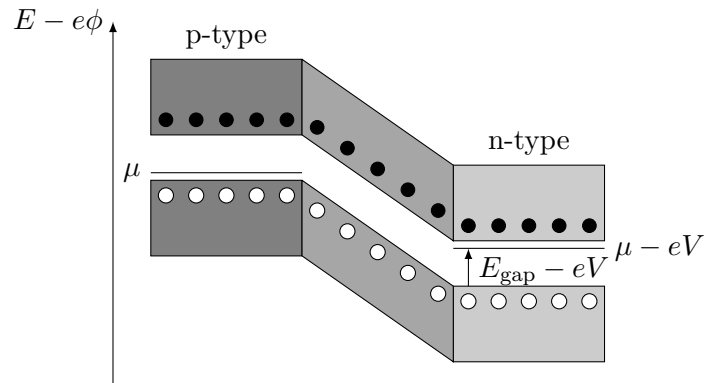

Figure 4: Energy band diagram of a reverse biased p-n junction.

The current-voltage characteristic of the p-n junction is described by the Schockley diode

equation,

$$I_{\text{diode}} = I_{\text{sat}}(T) \left(e^{eV/k_B T} - 1 \right),\tag{1}$$

wherein $I_{\text{sat}} \propto e^{-E_{\text{gap}}/k_B T}$ is the temperature dependent reverse bias saturation current and V the voltage applied to the p-n junction. Using the proportionality of the reverse bias saturation current, we can write,

$$I_{\text{diode}} \propto e^{(eV - E_{\text{gap}})/k_B T} - e^{-E_{\text{gap}}/k_B T},\tag{2}$$

which discloses the two effects contributing to the diode current. The left-hand side of the proportionality of Equation (2) represents the current contribution due intra-band excitation of charge carriers, whereas the right-hand side represents the current contribution due to inter-band excitation.
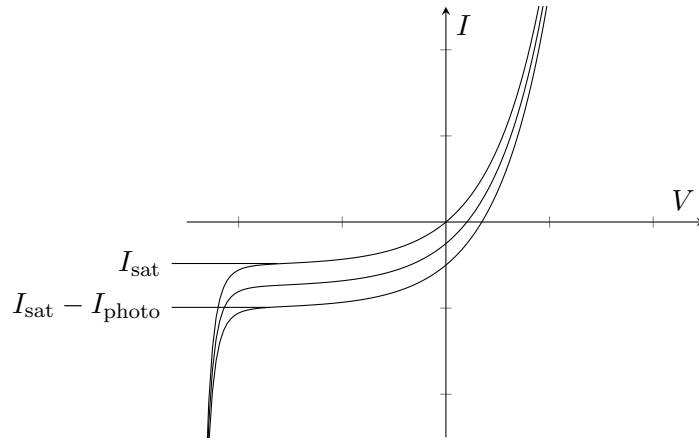

Figure 5: Current-voltage characteristics of a p-n junction with different levels of illumination.

In Figure 5 we see the current-voltage characteristics of the p-n junction under different levels of illumination. For negative voltages, the p-n junction is operated under reverse bias. If the reverse bias voltage exceeds the breakdown voltage the p-n junction starts to conduct. The current before the breakdown occurs is the reverse saturation current. For different levels of illumination, the curve is shifted downwards. The separation between the non-illuminated (top curve) and illuminated curves represent the respective photocurrent.

The conversion rate of photons to photoelectrons depends on the type of the band gap, i.e. direct or indirect, the wavelength λ of the photon and the temperature T. Most photodiodes report a wavelength λ dependent responsivity R which can be used to convert the radiant flux P of the incident light to the generated photocurrent I_{photo},

$$I_{\text{photo}} = RP.\tag{3}$$

For silicon-based p-n junctions, the responsivity R is between $0.2\,\mathrm{A\,W^{-1}}$ at $400\,\mathrm{nm}$ and $0.6\,\mathrm{A\,W^{-1}}$ at $950\,\mathrm{nm}$.
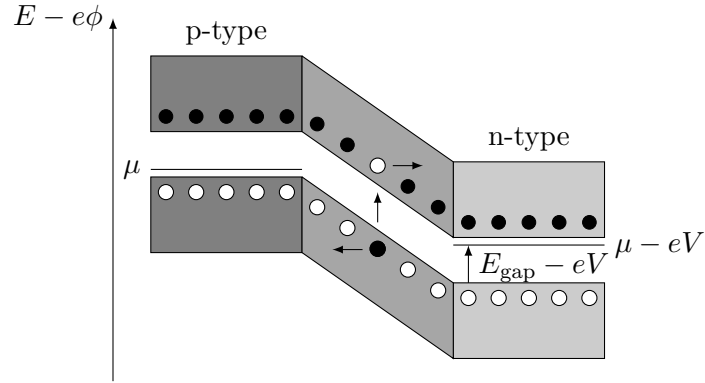

Figure 6: Energy diagram of a reverse biased p-n junction under illumination.

Figure 6 shows a p-n junction under reverse bias where a photon excites an electron-hole pair in the depletion region. Due to the electrostatic potential, the electron is accelerated to the right side. Analogue the hole is accelerated to the left side and in addition to the diode current, Equation (1), a photocurrent can be measured across the junction.

3.2 Lateral photoeffect

The lateral photoeffect was first discovered by W. Schottky in 1930 [3]. In 1957, it was rediscovered by J. Wallmark [4].
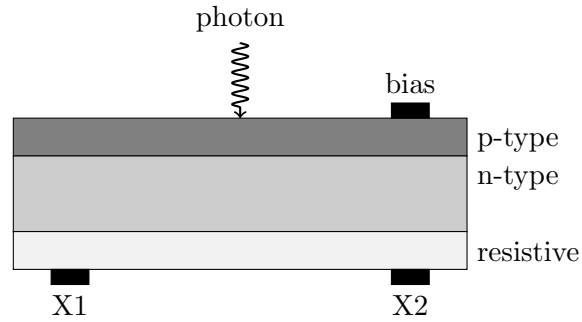

Figure 7: Cross section of a lateral photodiode.

$$\nabla^2 V = \frac{\rho}{w} J_s \left(e^{eV/k_B T} - 1 \right) - \frac{\rho_d}{w} J_p \tag{4}$$

8

$$\nabla^2 V \approx -\frac{\rho}{w}\left(J_s + J_p\right) \qquad\qquad \text{when } eV/k_B T \ll 1 \tag{5}$$

$$\nabla^2 V_p = -\frac{\rho_d}{w_d} J_p \tag{6}$$

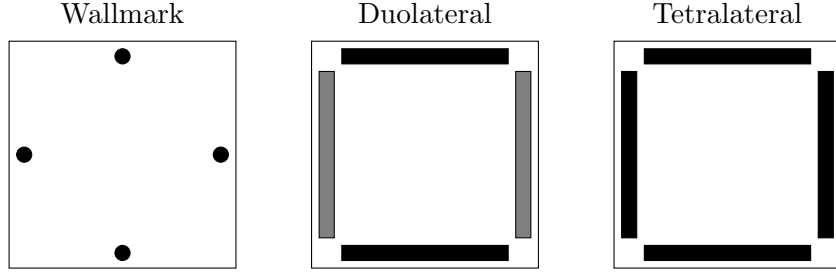$$V_p(x, y, t = 0) = I_p \frac{\rho}{w} \delta(x - x^*)\delta(y - y^*) \tag{7}$$

Figure 8: Contact configurations of a lateral photodiode.

$$V_{nm}^*(x, y) = \frac{\sin(m\pi x/l)\sin(n\pi y/l)}{(m^2 + n^2)\pi^2} l^2 \tag{8}$$

$$V_p^*(x, y) = I_p \frac{\rho}{w} \sum_{n\in\mathbb{Z}} \sum_{m\in\mathbb{Z}} \frac{\sin(m\pi x/l)\sin(m\pi x^*/l)\sin(n\pi y/l)\sin(n\pi y^*/l)}{(m^2 + n^2)\pi^2} \tag{9}$$

$$I_{x1}(x^*, y^*) = \frac{w}{\rho} \int_0^l \mathrm{d}y \left.\frac{\partial V}{\partial x}\right|_{x=0} \tag{10}$$

$$I_{x1}(x^*, y^*) = \frac{2}{\pi} I_p \sum_{n\in\mathbb{Z}} \frac{\sin[(2n-1)\pi y^*/l]}{2n-1} \frac{\sinh[|2n-1|\pi(1 - x^*/l)]}{\sinh(|2n-1|\pi)} \tag{11}$$

$$I_{x1}(x^*, l/2) = \frac{2}{\pi} I_p \sum_{n\in\mathbb{Z}} \frac{(-1)^{n+1}}{2n-1} \frac{\sinh(|2n-1|\pi(1 - x^*/l))}{\sinh(|2n-1|\pi)} \tag{12}$$

$$\approx I_p \left\{0.25 - 0.41731\left(\frac{x}{2l} - 1\right)\right\} + \mathcal{O}\left(\left(\frac{x^*}{l} - \frac{1}{2}\right)^2\right) \tag{13}$$

$$\frac{I_{x2}(x^*, l/2) - I_{x1}(x^*, l/2)}{I_{x1}(x^*, l/2) + I_{x2}(x^*, l/2)} \propto \frac{x}{l} \tag{14}$$

$$\frac{(I_{x2} + I_{y1}) - (I_{x1} + I_{y2})}{I_{x1} + I_{x2} + I_{y1} + I_{y2}} = \frac{2x}{l} \qquad \frac{(I_{x2} + I_{y2}) - (I_{x1} + I_{y1})}{I_{x1} + I_{x2} + I_{y1} + I_{y2}} = \frac{2y}{l} \tag{15}$$
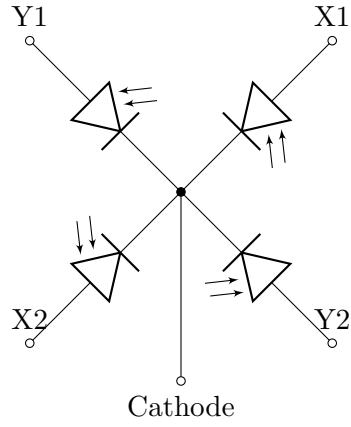
3.3 Characteristics

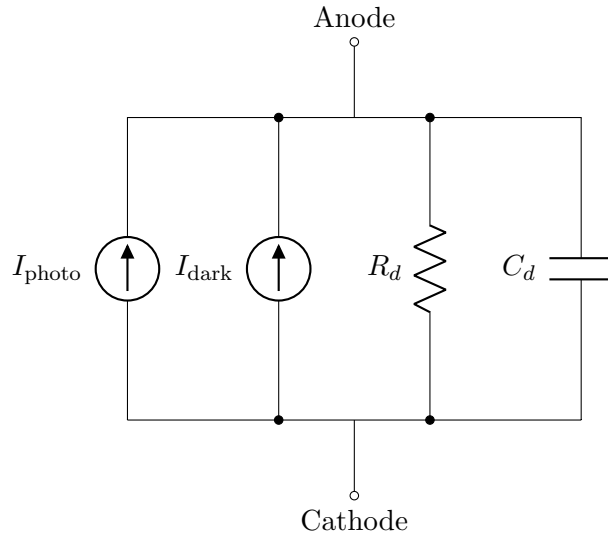Figure 9: Position-sensitive detector as photodiodes

Figure 10: Photodiode equivalent circuit

10

3.4 Noise and non-linear error

4 Preamplifier

The photocurrents created by our detector are in the range of microampere where they are vulnerable to noise. Using a preamplifier, we can increase the amplitude of the signal for an improved signal-to-noise ratio. The typical photocurrent preamplifier is based on the transimpedance (current-to-voltage) amplifier design using a voltage-feedback operational amplifier. Converting the current to a voltage signal has the benefit that the voltage signal can be easily visualized with an oscilloscope. Furthermore, the voltage-feedback operational amplifier design appears to be more common than the current-feedback operational amplifier, as manufacturers offer much more choice and they are more prominent in the literature. That said, current-feedback operational amplifiers are reported to be a viable solution for high-speed and high-bandwidth applications, see Ref. [5, p. 110] for an overview of the benefits of current-feedback amplifiers and Ref. [6, Ch. 9] for a comparison with voltage-feedback amplifiers. An embodiment of current-feedback operational amplifiers for high-accuracy applications can be found in Ref. [7, p. 143].

In the following, we will always refer to the voltage-feedback operational amplifier if not noted otherwise. Moreover, we expect the reader to be familiar with the foundations of the operational amplifier. Well-written introductions to this topic can be found in [5, Ch. 1] and [6, Ch. 3].

4.1 Basic design

The basic design of a transimpedance amplifier is illustrated in Figure 11. Ignoring imperfections of the photodiode, we can represent the photodiode as a current source. The non-inverting input of the operational amplifier is connected to ground. The inverting input is coupled with the output of the operational amplifier via a feedback impedance Z_f.
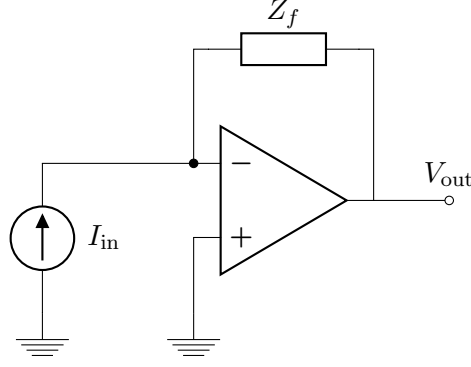
Figure 11: Basic transimpedance amplifier using voltage feedback operational amplifier.

The ideal operation amplifier has zero input current, thus, in the node of the inverting input of the operational amplifier Kirchhoff's law states that the current going through the feedback impedance has to cancel the current of the current source I_{in}. The current through the feedback impedance Z_f can be expressed in terms of the feedback impedance Z_f and the output voltage V_{out} of the operational amplifier through the use of Ohm's law, yielding,

$$V_{out} = -Z_f I_{in}. \tag{16}$$

Given a maximum current I_{in} and a desired maximum output voltage V_{out}, Equation (16) determines the feedback impedance. Limitations arise for real operational amplifiers where the output voltage is limited to be below the supply voltage of the operational amplifier.

Aside from photodiode applications, it is more common to find the inverting (voltage-to-voltage) operational amplifier in the literature. By using the source transformation on the current source with a parallel impedance in the transimpedance amplifier circuit, we can recover the inverting operational amplifier circuit, and thereby easily use results obtained for the inverting amplifier design.

(a) Transimpedance amplifier.
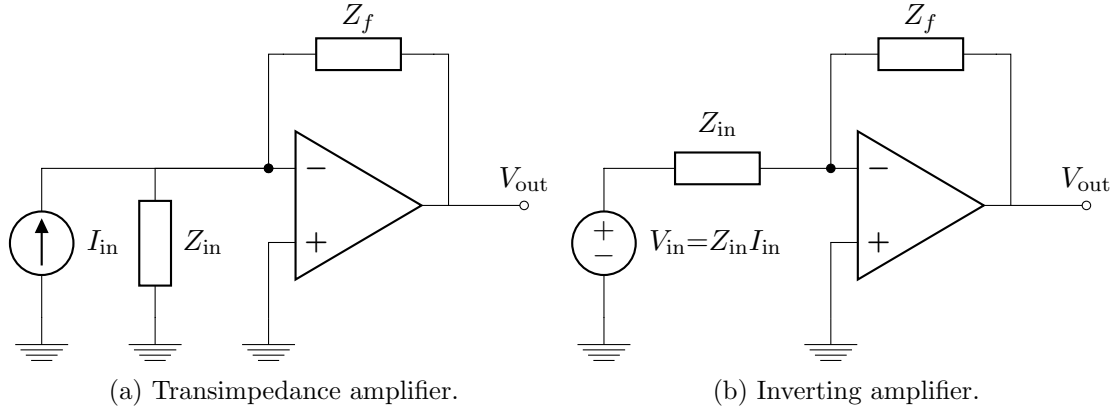(b) Inverting amplifier.

Figure 12: Equivalence between transimpedance and inverting amplifier using source transformation.

Figure 12 shows the source transformation applied to transimpedance and inverting amplifier circuits. Given a current source I_{in} with parallel impedance Z_{in} the equivalent voltage source has value $V_{\text{in}} = Z_{\text{in}}I_{\text{in}}$ with impedance Z_{in} in series.

4.2 Input offset voltage

Real operational amplifiers only reduce the voltage difference between the inverting and non-inverting input to a non-zero input offset voltage. For high-precision operational amplifiers, the input offset voltage is in the range of microvolts. We can model the input offset voltage as a voltage source at the non-inverting input of an ideal operational amplifier in our transimpedance circuit, as can be seen from Figure 13. In Figure 13 we amended the basic transimpedance circuit of Figure 11 by inserting a voltage source with the input offset voltage between the non-inverting input and ground.
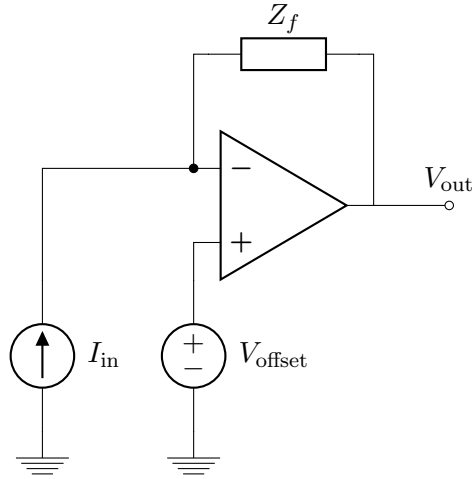
Figure 13: Input offset voltage in the transimpedance amplifier.

In order to estimate the output offset V_{out} caused by the input offset voltage V_{offset} we adapt the picture of the inverting amplifier. Figure 14 shows an inverting amplifier circuit with input impedance Z_{in} and input offset voltage V_{offset} at the non-inverting input of the operational amplifier. According to the superposition theorem, we can replace the input voltage source with a short circuit to estimate the contribution of the input offset voltage source.
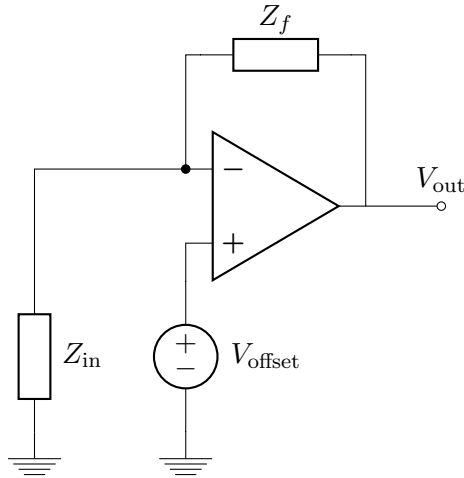

Figure 14: Input offset voltage in the inverting amplifier.

From Figure 14 we identify input and feedback impedance as a voltage divider in which

the input and output nodes are exchanged. The respective transfer function reads,

$$V_{\text{out}} = -\frac{R_f + R_{\text{in}}}{R_{\text{in}}} V_{\text{offset}} = -\left(1 + \frac{R_f}{R_{\text{in}}}\right) V_{\text{offset}}. \tag{17}$$

Comparing Equation (17) with Equation (16) discloses a difference in gain. The gain of the input signal in Eq. 1 is commonly referred to as signal gain. The gain of a signal applied directly to the inputs of the operational amplifier is referred to as noise gain. In the case of the position-sensitive detector, the input resistance is of order $10\,\text{k}\Omega$. Using a feedback resistance of $R_f = 100\,\text{k}\Omega$ we find that the input offset voltage experiences a gain of 11.

One approach to compensate for the input offset voltage as described is depicted in Figure 15, see also Ref [5, p. 54]. A potentiometer with maximum resistance Rp connects the positive and negative supply voltage. The wiper of the potentiometer is connected with a first resistor R1 to a node. The node is connected with a second resistor R2 and an optional bypass capacitor to ground. Finally, the equivalent input offset voltage source connects the node with the non-inverting input of the operational amplifier.
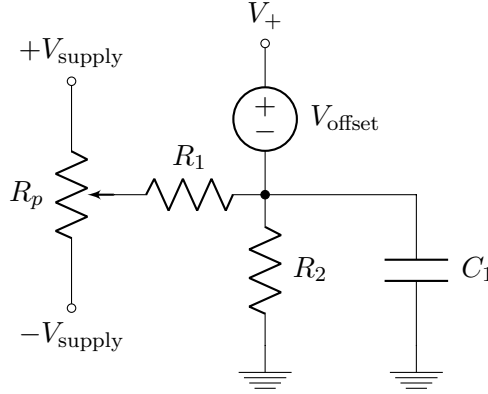

Figure 15: Input offset voltage compensation using adjustable potentiometer.

Let $0 \leq x \geq 1$ be the position of the potentiometer. For $x = 1/2$ the resistance of the potentiometer is $R_p/2$ and there is no offset compensation. For $x < 1/2$ the input offset compensation is negative to compensate for a positive input offset voltage. For $x > 1/2$ the input offset compensation is positive to compensate for a negative input offset voltage. The maximum input offset compensation is obtained for $x = 0$ and $x = 1$. Using circuit analysis techniques, we obtain,

$$V_c(x) = \frac{R_2(1 - 2x)}{R_1 + R_2 - R_p(1 - x)x} V_{\text{supply}}, \tag{18}$$

as an analytical expression for the input offset voltage compensation measured between the node and ground. The maximum absolute value of the compensation voltage follows

to be,

$$V_c(0) = V_c(1) = \pm \frac{R_2}{R_1 + R_2} V_{\text{supply}}. \tag{19}$$

Given a maximum input offset voltage of $100\,\mu\text{V}$ and a supply voltage of $15\,\text{V}$, we find approximate resistor values $R_1 = 3\,\text{M}\Omega$ and $R_2 = 2\,\Omega$. The resistor value of the potentiometer R_p should be chosen sufficiently large such to limit the current. For example, a potentiometer resistance of $R_p = 15\,\text{k}\Omega$ would limit the current to $2\,\text{mA}$ with a heat dissipation of $60\,\text{mW}$. In practice, one should aim for a slightly higher maximum compensation voltage in order to handle resistor mismatches.

That said, there are some practical arguments against the use of the described input offset voltage compensation. The first argument is that the low resistance of R_2 acts as a dominant source for thermal current noise density of about $100\,\text{pA}/\sqrt{\text{Hz}}$. As this current noise contributes to the input of the transimpedance amplifier it gets amplified by the feedback impedance Z_f, yielding up to $110\,\mu\text{V}/\sqrt{\text{Hz}}$ in voltage noise density, which — depending on the bandwidth — surpasses the actual input offset voltage to compensate. The second argument is that high-precision potentiometers with large dynamic range get very large and difficult to accommodate on a printed circuit board.

4.3 Input bias current

In addition to the input offset voltage V_{offset}, there is a second effect that causes an offset in the output voltage V_{out}. This second effect stems from the small amount of current that is drawn from the inputs of the operational amplifier. We highlighted the input currents in Figure 16 where they are represented by the current flows i_+ and i_- directly pointing into the inputs of the operational amplifier in the transimpedance circuit.
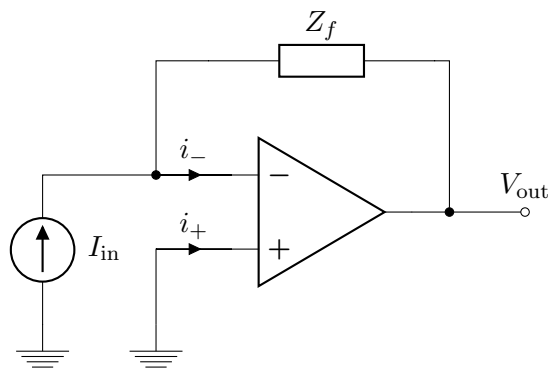

Figure 16: Input bias current offset in the transimpedance amplifier.

Input bias currents for high-precision operational amplifier are in the range of picoam-

peres. These small currents are usually difficult to measure and may differ between inputs. The datasheet of the operational amplifier, therefore, doesn't report the input bias current per terminal but the mean I_{bias} and the difference between the input currents I_{offset}. The relationship between the mean input bias current I_{bias} and the input offset current I_{offset} with respect to the actual input bias currents i_+, i_- is given below.

$$i_+ = I_{\text{bias}} + \frac{1}{2} I_{\text{offset}} \qquad\qquad I_{\text{offset}} = i_+ - i_- \tag{20}$$

$$i_- = I_{\text{bias}} - \frac{1}{2} I_{\text{offset}} \qquad\qquad I_{\text{bias}} = \frac{i_+ + i_-}{2} \tag{21}$$

According to Ref. [5, p. 57] and Ref. [8, p. 25] the effect of the input bias currents i_+, i_- on the output voltage V_{out} can be compensated with an impedance Z_c at the non-inverting input of the operational amplifier. Figure 17 illustrates the inverting amplifier configuration with such a compensation impedance Z_c.
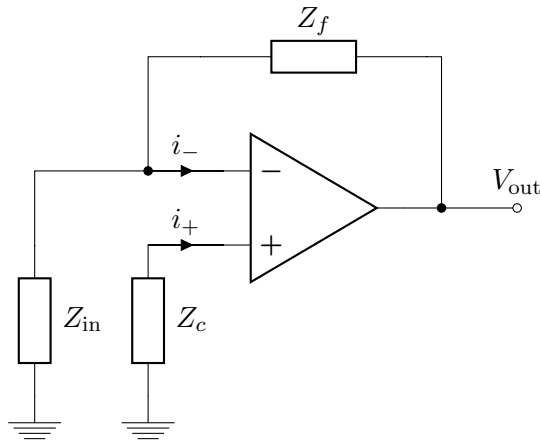

Figure 17: Input current offset compensation.

Following the argumentation from Ref. [9, p. 383], the input bias current at the inverting input of the operational amplifier i_- develops a voltage of $Z_f i_-$ over the feedback impedance Z_f. The input bias current at the non-inverting input i_- develops the voltage $Z_c i_-$ over the compensation resistor Z_c. The voltage $Z_c i_-$ propagates through the voltage divider comprising the feedback and input impedance analogue to the input offset voltage. According to the superposition theorem, both of these contributions add and yield,

$$V_{\text{out}} = i_+ Z_c \left(1 + \frac{Z_f}{Z_{\text{in}}} \right) - i_- Z_f, \tag{22}$$

at the output voltage. If $i_+ \approx i_-$ we can choose,

$$Z_c = \frac{Z_{\text{in}}}{Z_{\text{in}} + Z_f}, \tag{23}$$

18

to compensate for the output voltage offset caused by the input bias currents. The condition $i_+ \approx i_-$ is usually satisfied if the input offset current I_{offset} reported in the datasheet is less than the mean input bias current I_{bias}. High-precision operational amplifier usually have compensated bias currents that do not satisfy this condition. In this case, there is no generic formula for the value of the compensation impedance Z_c in terms of input and feedback impedance and one needs to perform impedance matching on a per-device basis. One should keep in mind that high-precision operational amplifier have input bias currents in the range of pA. Using Equation (22) one should therefore first check if the output voltage offset due to input bias currents is even worth compensating compared to other offset and noise contributions.

4.4 Stability and bandwidth

The outputs of the transimpedance and inverting amplifier designs have a phase shift of 180°. If an additional phase shift of 180° accumulates because of the inherent bandwidth limitations of the operational amplifier and the gain is equal or greater than unity, the conditions for oscillations are met and the amplifier will become unstable, see Ref. [9, p. 395]. By artificially limiting the bandwidth with an additional frequency pole, we can flatten out the frequency response at high frequencies, and thereby stabilize the amplifier, see Ref. [10, p. 184].

Figure 18 shows a Bode plot of the open-loop (black) and noise gain (red) of an operational amplifier. The noise gain separates into a compensated (solid) and uncompensated (dotted) branch.
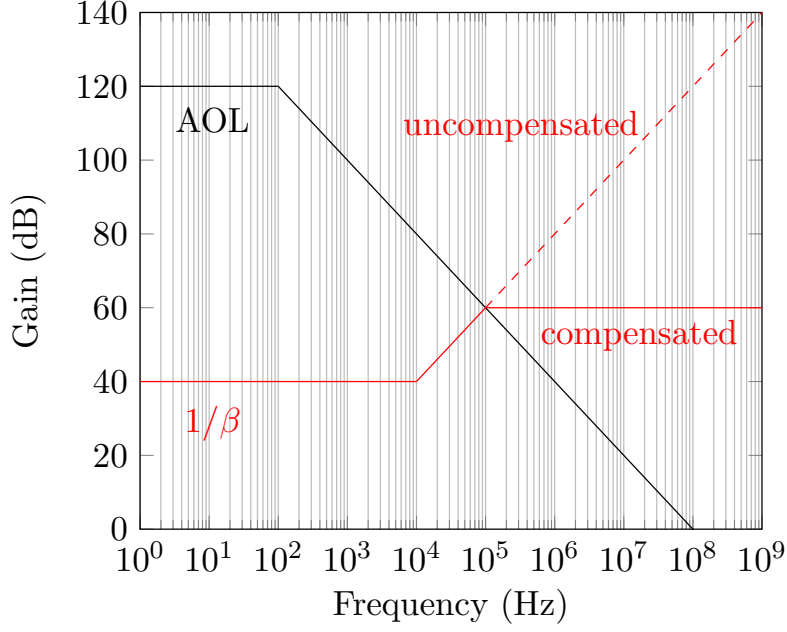
Figure 18: Bode plot of the open-loop and closed-loop gain of the amplifier.

With the uncompensated branch we would observe instability due to oscillations. The compensated branch is obtained through addition of a feedback capacitor. According to Ref. [5, p. 113], Ref. [11, p. 693] and Ref. [8, Ch. 3] the value for the feedback capacitance is given by,

$$C_f \geq \sqrt{\frac{C_{\text{in}}}{2\pi R_f f_u}}, \tag{24}$$

wherein R_f denotes the feedback resistance and f_u the unity-gain-bandwidth of the operational amplifier. The capacitance should be chosen larger to ensure design margin. The unity-gain-bandwidth of the operational amplifier denotes the frequency where the open-loop gain equals unity and is reported in the datasheet as gain-bandwidth-product (GBP) of the operational amplifier. C_{in} in Equation (24) represents the sum of the input capacities of the amplifier circuit and the capacitance of the signal source. According to Ref. [6, p. 185] a more exact formula for the feedback capacitance is given by,

$$C_f \geq \frac{C_{\text{aux}}}{2}\left(1 + \sqrt{1 + \frac{4C_{\text{in}}}{C_{\text{aux}}}}\right) \qquad\qquad C_{\text{aux}} = \frac{1}{2\pi R_f f_u}, \tag{25}$$

which is also valid if not $C_{\text{in}} \gg C_f$.

Figure 19 illustrates the transimpedance amplifier with capacitive elements. Parallel to the current source I_{in} we find the input capacitance C_{in} comprising source capacitance

and operational amplifier capacitance. Parallel to the feedback resistance R_f we find the feedback capacitance C_f with value given in Equation (25) or Equation (24).
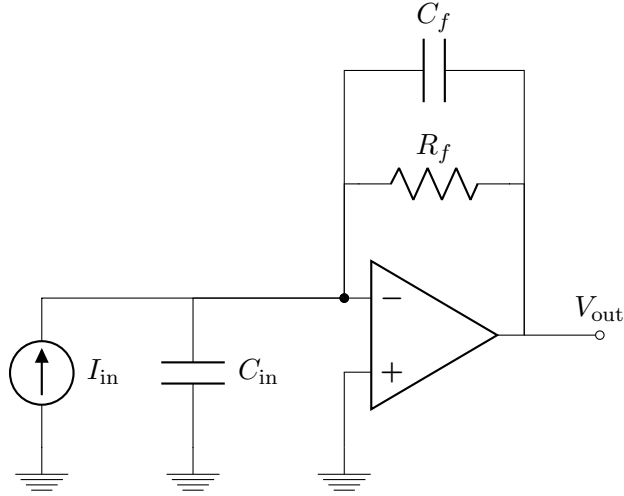

Figure 19: Transimpedance amplifier with capacitive elements.

As noted earlier, the bandwidth is reduced through the additional feedback capacitor. The new bandwidth is now given by the RC pole formed by the feedback impedance,

$$BW = \frac{1}{2\pi R_f C_f}. \tag{26}$$

Given a unity-gain-bandwidth of the operational amplifier of $f_u = 10\,\mathrm{MHz}$ and a feedback resistance of $R_f = 100\,\mathrm{k\Omega}$ Equation (24) yields a minimum feedback capacitance of $C_f = 4\,\mathrm{pF}$. Together with R_f this feedback capacitance limits the bandwidth to about $400\,\mathrm{kHz}$.

4.5 Noise density

Glossary

GBP gain-bandwidth-product. 20

References

[1] Anssi Mäkynen. "Position-sensitive devices and sensor systems for optical tracking and displacement sensing applications". PhD thesis. University of Oulu, 2000.

[2] Steven H. Simon. *The Oxford Solid State Basics*. OUP Oxford, 2013. ISBN: 9780199680771.

[3] Walter Schottky. "Über den Entstehungsort der Photoelektronen in Kupfer-Kupferoxydul-Photozellen". In: *Zeitschrift für Physik* 31 (Nov. 1930), pp. 913–925.

[4] J. T. Wallmark. "A New Semiconductor Photocell Using Lateral Photoeffect". In: *Proceedings of the IRE* 45.4 (Apr. 1957), pp. 474–483. DOI: 10.1109/JRPROC.1957.278435.

[5] Walt Jung. *Op Amp Applications Handbook*. Elsevier, 2005. ISBN: 9780750678445.

[6] Bruce Carter and Ron Mancini. *Op Amps for Everyone*. Elsevier, 2002. ISBN: 9780750677011.

[7] Date Noorlag. "Lateral-photoeffect position-sensitive detectors". PhD thesis. Delft University of Technology, 1974.

[8] Jerald Graeme. *Photodiode Amplifiers. Op Amp Solutions*. McGraw Hill Professional, 1996. ISBN: 9780070242470.

[9] David Terrel. *Op Amps. Design, Applications, and Troubleshooting*. Butterworth-Heinemann, 1996. ISBN: 9780750697026.

[10] Art Kay. *Operational Amplifier Noise. Techniques and Tips for Analyzing and Reducing Noise*. Elsevier, 2012. ISBN: 9780750685252.

[11] Philip Hobbs. *Building Electro-Optical Systems. Making it all Work*. John Wiley & Sons, 2011. ISBN: 9781118211090.